SMGroup

SM Journal of Biomedical Engineering

Research Article

Effect of Frequency and Focal Depth of Push Pulses on Acoustic Intensity, Mechanical Index, and Shear Wave Amplitude for Elastography Imaging

Seyedali Sadeghi[1], Sean Rothenberger[1], Dooman Akbarian[1] and Daniel H Cortes[1,2]*

[1]*Department of Mechanical Engineering, Pennsylvania State University, USA*
[2]*Department of Biomedical Engineering, Pennsylvania State University, USA*

Article Information

Received date: Jan 13, 2017
Accepted date: Feb 27, 2017
Published date: Mar 02, 2017

***Corresponding author**

Daniel H Cortes, Department of Biomedical Engineering and Mechanical Engineering, Pennsylvania State University, University Park, USA; Tel: 814-863-3103; E-mail: dhc13@psu.edu

Keywords Ultrasound shear wave elastography; Push pulse methods; FDA parameters; Shear waves; Axial particle velocity

Abstract

Over the past few years, there has been an increase on the application of Shear Wave Elastography (SWE) techniques to measure mechanical properties of musculoskeletal tissues for clinical applications. Imaging soft musculoskeletal tissues often requires the use of high frequency probes for high resolution at lower depths. The objective of this study is to measure the effect of frequency and focal depth on the acoustic output parameters (I_{SPPA}, I_{SPTA} and MI) as well as the amplitude of the generated shear waves by a 'push' pulse. To do this, acoustic output parameters were measured following NEMA guidelines. The frequency range used for the push pulses was 5-10MHz. The effect of frequency and focal depth on the amplitude of shear waves was evaluated on ultrasound phantom as well as on muscle and Achilles tendon. Acoustic output parameters and shear wave amplitude decreased as function of focal depth. However, the maximum acoustical intensity and the maximum displacement occurred at different frequencies. The maximum acoustic intensity was found at the center frequency of the transducer. These results shed light into the relationships between the properties of the ultrasound probe, acoustic output parameters, and shear wave amplitude for elastography applications.

Introduction

Shear Wave Elastography (SWE) is being used for measurement of mechanical properties of musculoskeletal tissues due to its potential for diagnosis of injuries or diseases in soft tissues. Often, high transducer frequencies (7-15 MHz) are used for ultrasound imaging of superficial and/or small musculoskeletal tissues; while lower frequencies (2-5 MHz) are employed for deeper tissues [1-6]. In order to use SWE in musculoskeletal tissues, such as tendon and ligaments, it may be necessary to use high frequency probes. However, current reports on acoustic output parameters (such I_{SPPA}, I_{SPTA} and MI) have been limited to lower frequencies [7-10]. Additionally, there is no information on the effect of frequency on the amplitude of the generated shear waves in musculoskeletal tissues.

Several SWE methods have been proposed for characterizing mechanical properties of soft tissues but all share a similar principle. ARFI measures mechanical properties by applying a focused push pulse and subsequently measuring the propagation of the generated shear wave using the same ultrasound probe [11-15]. Supersonic Shear Imaging (SSI) was developed by Bercoff et al. [16,17], in which a conical quasi-plane shear wave was produced by several focused 'push' pulses at different depths. An ultrafast plane wave imaging technique is needed so as to track shear wave motion generated. Comb-Push Ultrasound Shear Elastography (CUSE) was recently introduced by Song et al., in which the transducer elements are divided into subgroups which transmit ultrasound push pulses simultaneously [8,10]. A common characteristic of all these methods is that they use radiation force ('push' pulses) to generate shear waves followed by measuring pulses. Although the push and imaging pulses may use different frequencies, they have to be applied with the same probe. Therefore, the use of a particular probe may determine the frequency range used for the push pulses.

Currently, frequencies of 4-5 MHz are commonly used for the F-CUSE methods [9,10], while higher values (7-10 MHz) are employed for other methods such as SSI technique [16,17]. The FDA imposes limitations on the maximum values of acoustic output parameters for clinical use of elastography. These parameters include Spatial Peak Temporal Average Intensity (I_{SPTA}), Spatial Peak Pulse Average Intensity (I_{SPPA}), and Mechanical Index (MI) [18]. For elastography applications, the acoustic output parameters are typically close to the FDA limits. Therefore, it is important to understand the relationships between acoustic parameters, characteristics of the push pulses, and generated shear waves.

The objective of this study is to quantify the effect of the frequency and focal depth of the push pulses on the acoustic output parameters as well as amplitude of the generated shear

waves. The measurement procedures for obtaining acoustic output parameters were performed according to the National Electrical Manufacturers Association (NEMA) testing and labelling standard [19]. The relationships between the frequency and acoustic output parameters as well as amplitude of the generated wave presented in this manuscript may serve as guidelines for the development of SWE methods for musculoskeletal applications.

Methods

Acoustic intensity and mechanical index

FDA established limits on acoustic output parameters to avoid bioacoustics effects that are damaging to tissues [20]. These parameters include derated spatial peak time average intensity ($I_{SPTA,3}$), Derated Spatial Peak Pulse Average Intensity ($I_{SPPA,3}$), and Mechanical Index (MI). For musculoskeletal applications, the safety limits of these parameters are: $I_{SPTA.3} \leq 720$ mW/cm^2, and $I_{SPPA.3} \leq 190$ W/cm^2 or MI≤1.9. The measurements are derated by 0.3 dB cm^{-1} to consider the difference of in-tissue and in-water measurement effect. The maximum derated Pulse Intensity Integral ($PII_{.3}$) and the position at which it takes place, was determined by scanning the region of interest. The derated spatial-peak pulse-average intensity ($I_{SPPA.3}$) was calculated at the location of the maximum value of $PII_{.3}$ as Eqn 1 suggests:

$$I_{SPPA,3} = PII_{,3} / PD \quad (1)$$

where PD is pulse duration expressed in sec and the derated Pulse Intensity Integral is calculated as Eqn 2:

$$PII_{,3} = \exp(-0.23 * 0.3 * f_c * z) * PII \quad (2)$$

where z is the distance from the transducer assembly to the measurement point along the beam axis and f_c is the push pulse frequency expressed in MHz. The Pulse Intensity Integral (PII), which is equal to the energy flow per pulse, is the time integral of instantaneous intensity, for any specific pulse, integrated over the time interval in which the envelope of acoustic pressure for the specific pulse is nonzero and is calculated using the Eqn 3:

$$PII = \frac{\int_{t1}^{t2} V_h^2(t)\,dt}{10^4 \rho c M_L^2(f_c)} \quad (3)$$

where ρ is density (kg/m^3), c is the speed of sound (m/s), $M_L(f_c)$ is the hydrophone loaded sensitivity expressed in V/Pa and $v_h(t)$ is the output voltage of the hydrophone. The derated spatial-peak temporal-average intensity ($I_{SPTA.3}$) was calculated at the location of the maximum value of $PII_{.3}$ as Eqn 4:

$$I_{SPTA,3} = PII_{,3} * PRF \quad (4)$$

where PRF is the pulse repetition frequency in Hz. Finally, the MI gives an estimation of the risk of the non-thermal effects (cavitation and streaming) and is defined as Eqn 5:

$$MI = \frac{|p_{,3}|}{\sqrt{f_c}} \quad (5)$$

where $P_{.3}$ is the derated peak rarefaction pressure of the ultrasound wave (MPa) and is calculated as Eqn 6:

$$p_{,3} = \exp(-0.115 * 0.3 * f_c * z) * p \quad (6)$$

Experimental set-up

A Vantage 128 system (Verasonics, Inc., Edmond, WA) with a L11-4v probe was used for transmitting the push pulses. The probe was located perpendicular to the water surface in a water tank. The driving voltage and the number of push cycles were 50 V and 1000 cycles, respectively. This maximum driving voltage was selected since higher voltages did not result in increased values of acoustic intensity or mechanical index. This saturation effect may have been caused by a limitation on the amount of power delivered by the Vantage system. The tests were conducted with using 5 different frequencies including 5, 6.25, 7.3529, 8.9286 and 10.4167 MHz at several focal distances of the push cycles (5, 10, 15, 20, 25 and 30 mm). These frequencies were chosen to be in the -6 dB range of the ultrasound probe used (Figure 1).

Acoustic pressure was measured using a HGL-0200 hydrophone along with AH-2010-025 amplifier (ONDA Corp., Sunnyvale, CA). The hydrophone was attached to 3D positioning system with a spatial resolution of 0.1 mm. A MDO3012 oscilloscope (Tektronix Inc., Beaverton, OR, USA) with sampling rate of 2.5 GHz was used to record date from the Hydrophone. A Matlab (Mathworks, Natick, MA) script was coded to read the waveform directly from the oscilloscope and calculate the acoustic output parameters. Measurements were performed in a tank lined with 10 mm thick polyurethane acoustic absorber. De-ionized and degassed water at room temperature was used.

Particle axial velocity measurement

Particle velocity was used as an indicator of the amplitude of the shear waves generated at different frequencies and focal depths.

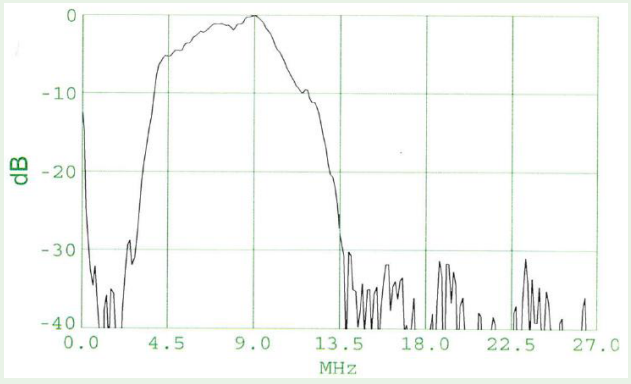

Figure 1: Sensitivity of the L11-4v transducer used for these measurements. The transducer -6 dB bandwidth is 4.11 to 10.59 MHz and its center frequency is 6.25 MHz.

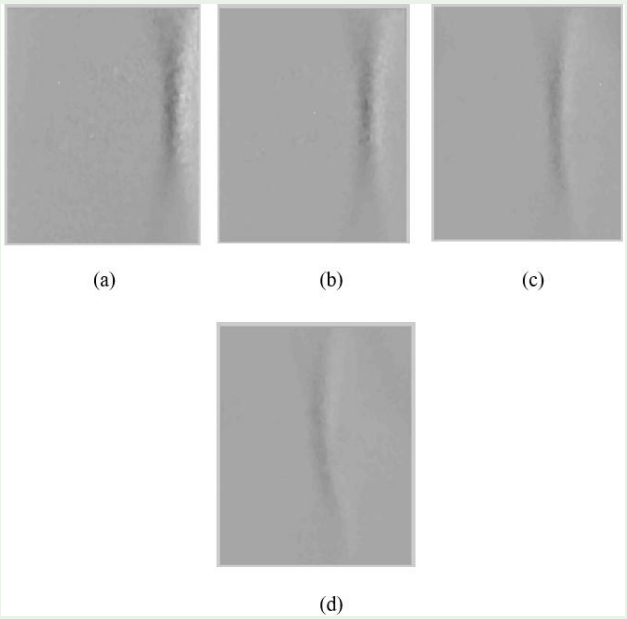

Figure 2: The experimental movie of shear wave propagation in Phantom at different time steps: (a) 0.5ms; (b) 1ms; (c) 2ms; (d) 3ms. The axial velocity was measured at the middle of the region of interest in the horizontal direction.

The particle velocity is the velocity experienced by a given point in the tissue when a shear wave passes through that location (it should not be confused with the shear wave speed). In general, the particle velocity is proportional to the shear wave amplitude. Particle velocity was measured in an elastography phantom (model 040, CIRS Inc., Norfolk, VA, USA), Rectus femoris muscle and Achilles tendon. The focal point was located at right edge of the region of interest. Therefore, shear waves can propagate from right to the left through the region of interest (Figure 2). A spatial median filter was employed to reduce the noise level. The axial velocity profile was used to measure the particle velocity in the horizontal direction at the focal depth, 1ms after the push pulse. In order to calculate the particle velocity, the frame derivative of the phase of the particles obtained by the Matlab, are converted to the time derivative of the particle displacement according to the Eqn 7:

$$V = \frac{d\theta}{dt} \cdot \frac{\lambda}{2\pi} \quad (7)$$

where $\frac{d\theta}{d}$ represents the time derivate of the phase of the particles and λ is the acoustic wave length at the frequency used for the imaging pulses (6.25 MHz).Measurements were conducted at different focal depths to evaluate the effect of frequency on shear wave amplitude at various focal depths for the phantom and muscle. Since the Achilles tendon thickness has a thickness of ~5 mm, the effect of focal depth was not evaluated in this tissue.

Figure 2: The experimental movie of shear wave propagation in Phantom at different time steps: (a) 0.5ms; (b) 1ms; (c) 2ms; (d) 3ms. The axial velocity was measured at the middle of the region of interest in the horizontal direction.

Table 1: The acoustic output parameters at the center frequency of 5 MHz.

Depth(mm)	MI	$I_{SPTA.3}$(mW/cm^2)	$I_{SPPA.3}$(W/cm^2)
10	1.8175	152.1	304.2959
15	1.6988	113.8	227.6404
20	1.4785	90.4	180.7663
25	0.9266	36.6	73.2732
30	0.68	24.4	48.7601

Table 2: The acoustic output parameters at the center frequency of 6.25 MHz.

Depth(mm)	MI	$I_{SPTA.3}$(mW/cm^2)	$I_{SPPA.3}$(W/cm^2)
10	1.6995	268.7	669.6111
15	1.4959	194.7	486.6365
20	1.2942	131.4	328.5751
25	0.921	79.2	198.0055
30	0.7086	26.6	110.72

Table 3: The acoustic output parameters at the center frequency of 7.3529 MHz.

Depth(mm)	MI	$I_{SPTA.3}$(mW/cm^2)	$I_{SPPA.3}$(W/cm^2)
10	1.5891	158.3	465.5486
15	1.3998	104.3	306.8046
20	1.0537	66.2	194.6624
25	0.6912	31.8	93.3846
30	0.5045	19.2	56.5311

Table 4: The acoustic output parameters at the center frequency of 8.9286 MHz.

Depth(mm)	MI	$I_{SPTA.3}$(mW/cm^2)	$I_{SPPA.3}$(W/cm^2)
10	1.3743	148.6	530.7752
15	1.1704	84.8	302.6946
20	0.8918	50.8	181.2846
25	0.5893	28.6	102.3134
30	0.396	14.8	52.8492

Table 5: The acoustic output parameters at the center frequency of 10.4167 MHz.

Depth(mm)	MI	$I_{SPTA.3}$(mW/cm^2)	$I_{SPPA.3}$(W/cm^2)
10	1.1416	86.4	359.8692
15	0.9912	60.3	251.2686
20	0.7032	30.2	126.0036
25	0.457	15.5	64.6714
30	0.3164	7.5	31.0436

Results

Acoustic intensity and MI results

The measured ultrasound acoustic intensity and MI are shown in Tables 1-5. MI and ISPTA.3values at various frequencies are below FDA regulatory limits. The maximum value of MI was found at a focal depth of 10 mm for a frequency of 5 MHz, while the maximum acoustic intensities ($I_{SPTA,3}$ and $I_{SPPA,3}$) were found at the same depth, but at the center frequency of the transducer.

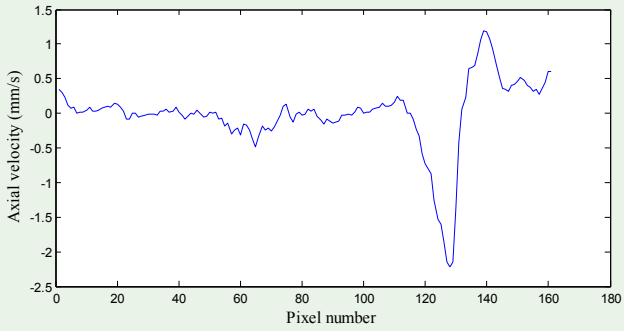

Figure 3: Axial velocity of phantom for 7.3529 MHz center frequency at the focal depth of 10 mm after 1 ms.

Table 6: Particle axial velocity values (mm/s) for various center frequencies at the different focal depths on phantom.

Focal Depth(mm)	Frequencies(MHz)				
	5.0000	**6.25**	**7.3529**	**8.9286**	**10.4167**
10	14.39	5.547	2.283	0.8808	0.6472
15	11.32	5.492	1.597	0.8128	0.5441
20	5.525	3.634	1.001	0.5571	0.5038
25	4.387	1.057	0.4467	1.193	-------
30	2.506	1.205	1.066	-------	-------

Table 7: Particle axial velocity values (mm/s) for various center frequencies at the different focal depths on rectus femorismuscle.

Focal Depth(mm)	Frequencies(MHz)				
	5.0000	**6.25**	**7.3529**	**8.9286**	**10.4167**
10	9.573	3.292	1.24	1.465	0.9416
15	6.818	2.02	1.12	1.1	0.5072
20	2.11	1.863	0.91	------	0.5
25	2.14	1.514	1.11	------	------
30	2.39	1.259	1.1	------	-------

Table 8: Particle axial velocity values (mm/s) for various center frequencies at the focal depth of approximately 10 mmin the Achilles tendon.

Frequencies(MHz)				
5.0000	**6.25**	**7.3529**	**8.9286**	**10.4167**
1.93	0.80	0.46	0.33	0.17

Axial velocity results

The particle axial velocity induced by shear wave propagation was calculated along the chosen focal point depths. An example of the particle velocity profile for a transducer frequency of 7.3529 MHz at a focal depth of 10 cm in the phantom is shown in Figure 3. The maximum axial velocities for various frequencies and focal depths on phantom, thigh muscle and Achilles tendon is expressed in Tables 6-8 respectively.

It is worth noting that some obtained values for maximum axial velocity at deeper focal distances at higher frequencies were noisy and not reliable, therefore, they are not reported.

Discussion

In this study, the effect of frequency and focal depth of push pulses on the acoustic intensity and MI as well as shear wave amplitude was analyzed. The acoustic parameters satisfied the FDA regulatory limits for the driving voltage and timing parameters used in this study. The FDA requires either the $I_{SPPA.3}$ or the MI to be under the regulated limits. In this case, the $I_{SPPA.3}$ exceeded the limit of 190 W/cm^2, but the MI for all experiments was under 1.9. Interestingly, the maximum acoustic intensity ($I_{SPPA.3}$) and the maximum axial velocity occurred at different frequencies. It was also observed that the Achilles tendon, which had the highest stiffness, resulted with the lowest axial velocity.

Several studies have reported acoustic output parameters for elastography methods. Tanter et al. [7] reported MI and ISPTA.3 values of 1.42 and 598 mW/cm^2 respectively, for the supersonic imaging elastography method. The frequency used for the SSI push pulse was 5 MHz, with a sonification time of 750 μs corresponding to 3,750 cycles. Although the MI and $I_{SPTA.3}$ were measured at several focal distances, only the 'worst case' values were reported at a focal depth of 20 mm. We measured a value of MI of 1.47 at 5 MHz and 20 mm (Table 1) which was very similar to that reported by Tanter et al. [7]. Their value of $I_{SPTA.3}$ was significantly higher than our value of 90.4 mW/cm^2 due to differences in the number of cycles (3,750 vs. 1,000) and possible differences in the pulse repetition rate. Song, et al. [9] reported $I_{SPPA.3}$, $I_{SPTA.3}$ and MI values109.4W/cm^2, 65.63mW/cm^2 and 0.9, respectively, for the Comb-Push Ultrasound Elastography (CUSE) method. A frequency of 4.09 MHz was used for the CUSE push pulse with a sonification time of 600 μs corresponding to 2454cycles. However, the CUSE method uses unfocused pulses. Therefore, the values of acoustic intensity and MI are much lower than those reported in this study and by Tanter et al. [7]. A focused CUSE (F-CUSE) method was later introduced by Song et al. [10]. A focal distance of 42 mm, frequency of 4.09 MHz and 2,454 cycles were used for the F-CUSE push pulses. For these parameters Song et al. [10] reported MI, $I_{SPTA.3}$ and $I_{SPPA.3}$ values of 0.45, 20.1 mW/cm^2, and 33.6 W/cm^2, respectively. Although their values of frequency and focal depth were outside the range considered for this study, the value of MI for our lowest frequency (5 MHz) and largest focal depth (30 mm) was 0.68. Therefore, it is reasonable to suggest that similar MI would have been obtained. Although different systems, probes, and parameters were used in our study and those of Tanter et al. [7] and Song et al. [10], there seems to be some consistency in the values of MI. Therefore, the values of MI reported in this study may serve as guidance for other systems and configurations.

The push-pulse frequency had a different effect on the MI, acoustic intensities and displacements. Not surprisingly, the MI was higher at lower frequencies and shorter focal depths. However, the acoustic intensities were higher at a different frequency. In our measurements the maximum $I_{sppa,3}$ occurred at the center frequency of the transducer (6.25 MHz). The second highest $I_{sppa,3}$ values were measured at 8.9289 MHz (10 mm focal depth) and corresponded to the peak sensitivity of the transducer (Figure 1). Since the voltage was maintained constant for these measurements, the results suggest that the sensitivity of the transducer may influence the results. Surprisingly, the maximum particle speed did not follow a similar trend as the acoustic intensity. The acoustic radiation force is proportional to the acoustic intensity [11]. Consequently, it was expected that particle velocity (or wave

amplitude) would follow the same trend as the intensity. However, higher particle velocities were measured at lower frequencies. A similar observation was reported by Carrascal et al. [21]. That study reported a decrease of shear wave amplitude as function of frequency in the range of 3-5 MHz. Carrascal, et al. considered the effect attenuation and phase aberration on shear wave amplitude and concluded that, at lower frequencies, attenuation is the most significant factor on the amplitude reduction. Similarly, Huang et al. [22] explored the effect of phase aberration in SWE, reporting that the phase aberration might not be the most influential factor on the performance of push pulse methods and reverberation and attenuation may play an important role in the amplitude of the shear waves as well. Conversely, Shi et al. [23] reported a decrease of shear wave amplitude, but suggested that phase aberration is more detrimental to shear wave amplitude than pure attenuation. Regardless of the most influential factor on the shear wave amplitude, the same trend was reported in all previous studies [21-23] which is in agreement with our results.

The particle velocity decreased with stiffness of the media. Particle velocity was measured in a phantom, rectus femoris muscle, and Achilles tendon with shear wave velocities of 2.65, 3.64, 16.75 m/s respectively. Our measurements showed that the particle velocity was lower in the Achilles tendon, which is stiffest medium tested. This result was expected since the radiation force produces smaller shear deformations in stiff media [11]. Additionally, we found that, for all media, the particle velocity drastically decreases as function of frequency. A two-fold increase in the frequency resulted in at least a 10-fold decrease in the particle velocity. While the radiation force increases linearly with absorption, the amplitude of the ultrasound waves decreases exponentially. This creates a challenging scenario for several orthopedic tissues. For instance, tendons and ligaments are better imaged width high-frequency probes (~10 MHz) and they also have a higher stiffness. That represents the worst combination for shear wave amplitude. This is clinically important, since it has been shown that error in the calculation of shear wave velocity are minimized when the shear wave amplitude is maximized [24]. The reduced amplitude of shear waves may be also related to the repeatability of elastography. An ex-vivo tendon study reported decreasing repeatability with increasing tendon load [25]. Tendon non-linearity causes an increased stiffness with loading and, consequently, decreased shear wave amplitude. In order to have low-frequency push pulses and high-frequency imaging acquisitions, SWE of stiff orthopedic tissues may benefit from technologies multi-frequency or ultra-broadband transducers [26,27].

There are several limitations in this study. The obtained acoustic output parameters were measured using only one transducer. Transducer with different sensitivities may produce different results. However, the frequency and stiffness effects on the parameter measured are independent of the transducer used. Additionally, the comparison of acoustic output parameter with those reported in literature suggests that MI values are consistent across different systems and transducers. Another limitation is that the particle velocity was not measured at the focal point. This is a limitation of any ultrasound system with a single ultrasound transducer. Since there is a delay between the end of the push pulse and the first images obtained for measuring displacements, a small amount of wave propagation is expected in that time. Carrascal et al. [21] employed two linear array transducers opposed to each other on two opposite sides of the phantom in order to capture the shear wave displacement at the focal point. However, since most clinical ultrasound scanners operate with one transducer at the time, the results shown here are representative for those systems.

In conclusion, higher shear wave amplitudes were generated at the lowest frequency tested of the push pulses, but the maximum acoustic intensity was found at the center frequency of the transducer. The stiffness of the medium appeared to be influential on the shear wave amplitude as particle axial velocities. Future work will include the analysis of transducer impedance and transduction efficiency on acoustic output parameters and quality of shear wave elastograms.

Acknowledgement

This study was financed by the Pennsylvania State University through start-up funds.

References

1. Shiina T, Nightingale KR, Palmeri ML, Hall TJ, Bamber JC, Barr RG, et al. WFUMB guidelines and recommendations for clinical use of ultrasound elastography: Part 1: basic principles and terminology. Ultrasound Med Biol. 2015; 41: 1126-1147.
2. Cosgrove D, Piscaglia F, Bamber J, Bojunga J, Correas JM, Gilja O, et al. EFSUMB guidelines and recommendations on the clinical use of ultrasound elastography. Part 2: Clinical applications. Ultraschall Med. 2013; 34: 238-253.
3. Ferraioli G, Filice C, Castera L, Choi BI, Sporea I, Wilson SR, et al. WFUMB guidelines and recommendations for clinical use of ultrasound elastography: Part 3: liver. Ultrasound Med Biol. 2015; 41: 1161-1179.
4. Sarvazyan A, Hall TJ, Urban MW, Fatemi M, Aglyamov SR, Garra BS. An overview of elastography - An emerging branch of medical imaging. Curr Med Imaging Rev. 2011; 7: 255-282.
5. Gennisson JL, Deffieux T, Fink M, Tanter M. Ultrasound elastography: principles and techniques. Diagn Interv Imaging. 2013; 94: 487-495.
6. Sarvazyan AP, Rudenko OV, Swanson SD, Fowlkes JB, Emelianov SY. Shear wave elasticity imaging: a new ultrasonic technology of medical diagnostics. Ultrasound Med Biol. 1998; 24: 1419-1435.
7. Tanter M, Bercoff J, Athanasiou A, Deffieux T, Gennisson J-L, Montaldo G, et al. Quantitative assessment of breast lesion viscoelasticity: initial clinical results using supersonic shear imaging. Ultrasound Med Biol. 2008; 34: 1373-1386.
8. Mehrmohammadi M, Song P, Meixner DD, Fazzio RT, Chen S, Greenleaf JF, et al. Comb-push ultrasound shear elastography (CUSE) for evaluation of thyroid nodules: preliminary in vivo results. IEEE Trans Med Imaging. 2015; 34: 97-106.
9. Song P, Zhao H, Manduca A, Urban MW, Greenleaf JF, Chen S. Comb-push ultrasound shear elastography (CUSE): a novel method for two-dimensional shear elasticity imaging of soft tissues. IEEE Trans Med Imaging. 2012; 31: 1821-1832.
10. Song P, Urban MW, Manduca A, Zhao H, Greenleaf JF, Chen S. Comb-push ultrasound shear elastography (CUSE) with various ultrasound push beams. IEEE Trans Med Imaging. 2013; 32: 1435-1447.
11. Nightingale KR, Palmeri ML, Nightingale RW, Trahey GE. On the feasibility of remote palpation using acoustic radiation force. J Acoust Soc Am. 2001; 110: 625-634.
12. Nightingale K, McAleavey S, Trahey G. Shear-wave generation using acoustic radiation force: in vivo and ex vivo results. Ultrasound Med Biol. 2003; 29: 1715-1723.
13. Lupsor M, Badea R, Stefanescu H, Sparchez Z, Branda H, Serban A, et al. Performance of a new elastographic method (ARFI technology) compared to unidimensional transient elastography in the noninvasive assessment of

chronic hepatitis C. Preliminary results. J Gastrointestin Liver Dis. 2009; 18: 303-310.

14. Sporea I, Sirli R, Popescu A, Danilă M. Acoustic Radiation Force Impulse (ARFI)--a new modality for the evaluation of liver fibrosis. Med Ultrason. 2010; 12: 26-31.

15. Kiani A, Brun V, Lainé F, Turlin B, Morcet J, Michalak S, et al. Acoustic radiation force impulse imaging for assessing liver fibrosis in alcoholic liver disease. World J Gastroenterol. 2016; 22: 4926-4935.

16. Bercoff J, Tanter M, Fink M. Supersonic shear imaging: a new technique for soft tissue elasticity mapping. IEEE Trans Ultrason Ferroelectr Freq Control. 2004; 51: 396-409.

17. Athanasiou A, Tardivon A, Tanter M, Sigal-Zafrani B, Bercoff J, Deffieux T, et al. Breast lesions: quantitative elastography with supersonic shear imaging-preliminary results. Radiology. 2010; 256: 297-303.

18. Medicine AIoUi. Safety standard for diagnostic ultrasound equipment. J Ultrasound Med. 1983; 2: 1-50.

19. Medicine AIoUi, Association NEM. Acoustic output measurement standard for diagnostic ultrasound equipment. Laurel MD: American Institute of Ultrasound in Medicine. 1998.

20. Food and Drug Administration. Information for manufacturers seeking marketing clearance of diagnostic ultrasound systems and transducers. Rockville MD: Center for Devices and Radiological Health, US Food and Drug Administration. 1997.

21. Carrascal CA, Aristizabal S, Greenleaf JF, Urban MW. Phase Aberration and Attenuation Effects on Acoustic Radiation Force-Based Shear Wave Generation. IEEE Trans Ultrason Ferroelectr Freq Control. 2016; 63: 222-232.

22. Huang SW, Xie H, Robert J-L, Nguyen M, Shamdasani V. Phase aberration in ultrasound shear wave elastography-impacts on push and tracking. Ultrasonics Symposium (IUS), 2016 IEEE International. 2016.

23. Shi Y, Xie H, Shamdasani V, Fraser J, Robert J-L, Zhou S, et al. Phase aberration in shear wave dispersion ultrasound vibrometry. Ultrasonics Symposium (IUS), 2011 IEEE International. 2011.

24. Urban MW, Chen S, Greenleaf JF. Error in estimates of tissue material properties from shear wave dispersion ultrasound vibrometry. IEEE Trans Ultrason Ferroelectr Freq Control. 2009; 56: 748-758.

25. Peltz C, Haladik J, Divine G, Siegal D, van Holsbeeck M, Bey M. ShearWave elastography: repeatability for measurement of tendon stiffness. Skeletal Radiol. 2013; 42: 1151-1156.

26. Martin KH, Lindsey BD, Ma J, Lee M, Li S, Foster FS, et al. Dual-frequency piezoelectric transducers for contrast enhanced ultrasound imaging. Sensors. 2014; 14: 20825-20842.

27. Akiyama I, Saito S, Ohya A. Development of an ultra-broadband ultrasonic imaging system: Prototype mechanical sector device. J Med Ultrason. 2006; 33: 71-76.